Research Article

Sciences of Pharmacy

Ethanol Extract of Grass Jelly Leaves: Bioactive Analysis and *In silico* Study on Estrogen Receptor Alpha Related to MCF-7 Breast Cancer

Abdul Mulki Irpani, Anne Yuliantini, Muhammad Ilham Bintang, Arinda Tri Pramay Sella, Jajang Japar Sodik

[The author informations are in the declarations section. This article is published by ETFLIN in Sciences of Pharmacy, Volume 5, Issue 3, 2026, Page 312-322. DOI: 10.58920/sciphar0502619]

Received: 26 February 2026
Revised: 29 April 2026
Accepted: 21 June 2026
Published: 20 July 2026

Editor: Rina Wijayanti

Keywords: Breast cancer, Grass jelly, In silico, LC-HRMS, MCF-7..

Abstract: Breast cancer is a major cause of mortality among women and requires the development of alternative therapies derived from natural products. This study aimed to profile bioactive compounds in the ethanol extract of gras jelly leaves (*Cyclea barbata* Miers) and evaluate their predicted interactions with estrogen receptor alpha (ERα), a key regulator of proliferation in ER-positive MCF-7 breast cancer cells using an *in silico* approach. LC–HRMS analysis followed by database matching tentatively annotataed 44 major compounds based on peak intensity after data filtering. Molecular docking and simulation results indicated that several compounds exhibited favorable predicted binding affinity toward estrogen receptor targets. Among them, (3β, 24R, 24′R)-fucosterol epoxide demonstrated the most stable interaction. These findings suggest that the compound showed promising interaction stability toward the estrogen receptor in computational analysis. However, further *in vitro* and *in vivo* studies are required to validate its biological activity

Introduction

The World Health Organization (WHO), through the International Agency for Research on Cancer (IARC), reported that the global cancer burden has reached approximately 20 million cases across 185 countries. Among these, breast cancer accounts for 11.6% of cancer-related deaths, ranking second worldwide. According to Global Cancer Statistics 2020, breast cancer ranks first in cancer incidence in Indonesia. Cancer is a chronic disease characterized by abnormal cellular changes leading to uncontrolled cell growth and proliferation, with the potential to metastasize (1, 2). Breast cancer is a malignant tumor arising from breast tissue and remains one of the most feared diseases among women (3).

As a country with high biodiversity, Indonesia has significant potential for the development of natural products that remain underutilized in modern medicine (4). Numerous indigenous plants contain bioactive compounds with pharmacological activities, including anti-breast cancer properties (5). One plant with potential for development as a source of bioactive compounds is *Cyclea barbata* Miers. This plant is known to contain various secondary metabolites, such as flavonoids, alkaloids, and phenolic compounds, which have been reported to have antioxidant activity, and can be used to treat fever, gastritis, hypertension, diarrhea, coughing, nausea, and digestive disorders (6). Previous studies have shown that Green Grass Jelly leaves contain various bioactive compounds, including flavonoids, alkaloids, tannins, and saponins (6). The flavonoid content, in particular, has demonstrated potential as an anticancer agent (7). These compounds have been reported to exhibit diverse pharmacological activities, such as antibacterial and antioxidant effects. Furthermore, Green Grass Jelly leaves have shown cytotoxic potential against cancer cells (6). Because estrogen receptor alpha (ERα) plays a central role in the proliferation and progression of ER-positive breast cancer cells, investigating the interaction of Green Grass Jelly leaves metabolites with this receptor may provide mechanistic insight into the previously reported cytotoxic activity of the plant. However, studies investigating the potential of active compounds from Green Grass Jelly leaves against MCF-7 breast cancer cells through *in silico* approaches remain limited. *In silico* methods employing molecular computational techniques, such as molecular docking, enable the prediction of compound–target protein binding affinity in cancer cells efficiently and accurately. This approach represents an important preliminary step in the discovery and development of natural product–based anticancer agents (8, 9).

Given the high prevalence of breast cancer, the exploration of natural bioactive compounds as alternative therapeutic candidates remains an important area of research. The search for and development of safer and more effective therapeutic agents through the utilization of natural bioactive compounds is therefore essential. Considering the bioactive potential of green grass jelly leaves, this plant may serve as a potential source of compounds for breast cancer-related research. Accordingly, this study aims to analyze the active compounds present in the ethanolic extract of Green Grass Jelly leaves and to evaluate their potential as anticancer agents against MCF-7 breast cancer cells using an *in silico* approach. MCF-7 is an estrogen receptor-positive breast cancer cell line, making ERα a biologically relevant molecular target for computational screening.

Although Green Grass Jelly leaves have been reported to possess antioxidant and cytotoxic properties, studies investigating its metabolite profile and predicted interaction against ERα using integrated LC–HRMS and molecular simulation approaches remain limited. Therefore, we hypothesized that bioactive compounds present in Green Grass Jelly leaves may exhibit favorable interactions with ERα and could contribute to the previously reported cytotoxic activity of the plant. Accordingly, this study aims to analyze the active compounds present in the ethanolic extract of Green Grass Jelly leaves and evaluate their potential interactions with ERα using an *in silico* approach.

Experimental Section

Preparation of *Simplisia*

A total of 2000 g of Green Grass Jelly leaves (*C. barbata* Miers) were collected, followed by wet sorting and washing under running water. The samples were then dried in a drying oven (Memmert, Germany) at 60 °C for 10–24 h. The dried material was re-sorted, ground using a blender (Philips, Indonesia), and sieved through a 60-mesh sieve to obtain a homogeneous *simplisia* powder (10).

Simplisia Extraction

Extraction was carried out using the maceration method. A total of 100 g of simplisia powder was macerated with 1000 mL of 96% ethanol (Merck, Germany) for 3 days, with stirring every 24 h. The filtrate was filtered using Whatman No. 1 filter paper, and the solvent was replaced for remaceration. All filtrates were combined and concentrated using a rotary evaporator (Büchi R-300, Flawil, Switzerland) at a pressure of 175–180 mBar and a temperature of 55 °C. The concentrated extract was stored at 4 °C until further use (11, 12).

Phytochemical Screening

The phytochemical test solution was prepared by dissolving 200 mg of the extract sample in 25 mL of 70% ethanol. Each test was performed in triplicate (13). Preliminary phytochemical screening was conducted using standard qualitative procedures to tentatively detect the presence of major secondary metabolite groups, including alkaloids, flavonoids, tannins, quinones, steroids, and terpenoids. However, these screening methods provide only an initial indication of phytochemical constituents and were not fully validated or quantitatively assessed.

Extract Profiling

The extract profile was monitored using Thin Layer Chromatography (TLC) with silica gel GF_{254} (Merck, Darmstadt, Germany) as the stationary phase. The mobile phase was adjusted according to the polarity of the target compounds. TLC plates were observed under UV light at 254 and 366 nm (Camag UV Lamp, Switzerland). Spot-detecting reagents included 10% H_2SO_4 in methanol (universal reagent), Liebermann–Burchard reagent (for triterpenoids), and 5% $AlCl_3$ in methanol (for flavonoids).

Metabolite Profiling by LC–HRMS

Identification of bioactive compounds was carried out using Liquid Chromatography–High Resolution Mass Spectrometry (LC–HRMS) with a Q-Exactive Orbitrap™ system (Thermo Fisher Scientific, Bremen, Germany). The acquired spectral data were processed and matched against reference databases using accurate mass measurements, isotopic patterns, and MS/MS fragmentation spectra for tentative compound identification. Putative identifications were supported by comparison of fragmentation patterns with spectral libraries; however, no authentic reference standards were used for confirmation, and therefore the reported compounds should be considered as tentatively identified. Compound annotation confidence levels were assigned based on the Metabolomics Standards Initiative (MSI), with most features corresponding to Level 2 identification.

The identified metabolites included phenolic compounds, flavonoids, alkaloids, and terpenoids, which are commonly reported to possess antioxidant and antidiabetic activities. These results provide a preliminary phytochemical profile of the ethanolic extract of Green Grass Jelly leaves.

In silico Study

The *in silico* study was conducted using molecular docking and molecular dynamics simulations. The workflow included ligand preparation, protein preparation, validation of the molecular docking method, docking simulation of test ligands with target proteins, visualization, molecular dynamics simulation, and result interpretation. The molecular docking system was run on a Linux Ubuntu 24.04 LTS operating system with a Ryzen 7 5700X CPU, GeForce RTX 3070 Ti 8 GB GPU, 32 GB RAM, and 8.5 TB storage. The software utilized included Autodock Tools 4.2.3 (The Scripps Research Institute, La Jolla, CA, USA), MGLTools 1.5.6, GROMACS 2024 (University of Groningen, Netherlands), AmberTools 2024, PyRx 0.9.2 (Molecular Graphics Laboratory, USA), Discovery Studio Visualizer 2025 (BIOVIA, San Diego, USA), VMD (Visual Molecular Dynamics, University of Illinois, USA), XTB 6.4.1, RDKit, Protein-Ligand Interaction Profiler (PLIP) Version 2.3.1, and ChemBio Office 2016.

Protein Crystal Structures

Protein Crystal Structures High-resolution, non-mutant crystal structures of the following proteins from the receptors were obtained from the RCSB Protein Data Bank. The crystal structure of Estrogen Receptor Alpha (ERα) with PDB ID: 7NDO was obtained from the RCSB Protein Data Bank. This structure was selected because it represents the ligand-binding domain of ERα, a transcription factor involved in estrogen-mediated

signaling and a validated therapeutic target for hormone-dependent diseases. Furthermore, the crystal structure was determined by X-ray diffraction at a high resolution of 1.60 Å, providing highly accurate atomic coordinates suitable for molecular docking studies.

Protein Structure Preparation

The crystal structure of Estrogen Receptor Alpha (ERα) was retrieved from the RCSB Protein Data Bank (PDB ID: 7NDO). Water molecules and non-protein residues were removed using Discovery Studio to isolate the macromolecule for docking (15).

Ligand Structure Preparation

Ligand structures were retrieved from the PubChem database using SMILES strings derived from the LC–HRMS analysis. The 2D structures were converted to 3D, followed by geometry optimization using the xTB (eXtended Tight-Binding) software, utilizing the GFN-xTB method.

Molecular Docking Analysis

Molecular docking validation was performed using AutoDock version 4.2.3 (20) on the prepared protein. The natural ligand was separated from the protein using Discovery Studio and then re-docked to the target protein (redocking). The center of the grid was positioned within the natural ligand, encompassing all residues in the binding site. Grid box determination was achieved by identifying the central region of the natural ligand and performing docking with a maximum of 100 GA runs (medium evals) using the Lamarckian Genetic Algorithm (LGA). The validation was considered successful if the Root Mean Square Deviation (RMSD) value was ≤ 2Å (21). Docking simulations of the test ligands against the target protein were performed using the AutoDock4 algorithm implemented in PyRx 0.9.2, utilizing grid box settings obtained from the validation results. The final stage involved interpreting the molecular docking results by analyzing the ΔG (binding free energy) values and intermolecular interactions (22).

Molecular Dynamics Simulation

Molecular dynamics simulations were performed using the GROMACS version 2024 application (https://www.gromacs.org/) to simulate the interaction between the target and ligand under conditions approximating the physiology of the organism. The modeling phase involved topology preparation, including 7NDO target preparation, topology ligand preparation, protein and ligand solvation stages using a box-type simulation, energy minimization to avoid unwanted contact between atoms, and equilibration to maintain constant temperature, pressure, and volume throughout the simulation. Equilibration was performed to regulate the system temperature at the desired level, e.g., a constant temperature of 310K. The total number of protein and ligand atoms was also calculated in the s line of the complex. gro file. MD simulations were performed for 100 ns. The trajectories were analyzed to assess the stability and conformational behavior of the protein–ligand complex under physiological conditions, The protein was parameterized with the AMBER ff13SB force field, which has been widely validated for reproducing protein structural dynamics and stability. Prior to the production run, the system underwent energy minimization followed by equilibration under NVT and NPT ensembles. After the trajectories was completed, the final stage was to analyze the results of the molecular dynamics simulation, including RMSD, RMSF, hydrogen bonding, and MMGBSA.

Results and Discussion

In the first stage, extraction was carried out using the maceration method, which does not require heating and thus minimizes the degradation of thermolabile compounds. The yield data are summarized in **Table 1**. Drying 2,000 g of fresh grass jelly leaves produced 263.11 g of dried plant material (simplicia), corresponding to a yield of 13.16%, whereas maceration of 100 g of simplicia produced 23.08 g of concentrated ethanolic extract, corresponding to an extraction yield of 23.08%. The reduction in mass during simplicia preparation primarily reflects moisture removal, while the extract yield represents the proportion of ethanol-soluble constituents recovered from the dried material.

The solvent used was 96% ethanol, due to its suitable polarity and status as a universal solvent capable of extracting a wide range of chemical compounds, from polar to non-polar. Additionally, ethanol is less prone to

Table 1. Yield of *simplisia* and extract of Green Grass Jelly leaves.

Plant Material	Sample Weight (g)	Dried Weight (g)	Yield (%)
Simplisia	2,000	263.11	13.155
Ekstrak	100	23.08	23.08

Table 2. Phytochemical screening results of Green Grass Jelly leaves.

Secondary Metabolite	*Simplisia*	Extract
Alkaloid	+	+
Steroid/Triterpenoid	+	+
Kuinon	-	-
Flavonoid	+	+
Saponin	+	-
Tannin	+	+

microbial contamination and is considered less toxic compared to other organic solvents (14).

In the second stage, phytochemical screening was conducted on both the *simplisia* and the ethanolic extract of Green Grass Jelly leaves (*C. barbata* Miers), and the results are summarized in **Table 2**. The choice of solvent in the extraction process generally follows the principle that nonpolar compounds dissolve in nonpolar solvents, whereas polar compounds dissolve in polar solvents. This directly affects the chemical constituents that can be extracted, depending on the solvent's polarity (15).

As shown in **Table 2**, phytochemical screening confirmed the presence of alkaloids, flavonoids, tannins, and steroid/triterpenoid constituents in both the simplicia and ethanolic extract. While these metabolite classes have previously been reported in *C. barbata* Miers, their detection in the present extract supports the suitability of ethanol as an extraction solvent for recovering compounds potentially relevant to biological activity. The persistence of these metabolite groups after extraction suggests that ethanol efficiently extracted semi-polar constituents that may contribute to the pharmacological properties previously reported for this plant.

Among the detected metabolite classes, flavonoids and triterpenoids are particularly relevant because several compounds belonging to these groups have been reported to interact with signaling pathways associated with cancer progression, including estrogen receptor-mediated mechanisms. Nevertheless, phytochemical screening provides only qualitative information and does not allow direct attribution of biological activity to specific constituents. Therefore, further metabolite profiling using LC–HRMS was required to obtain a more detailed characterization of the extract composition.

Meanwhile, quinones were not detected in either the *simplisia* or the ethanolic extract, and saponins were only present in the *simplisia* but absent after extraction. The loss of saponins in the ethanolic extract is likely due to their higher solubility in polar solvents such as water compared to ethanol, resulting in suboptimal extraction. Overall, these results indicate that the ethanol extraction method is capable of isolating most of the active secondary metabolites, particularly semi-polar compounds such as flavonoids and alkaloids, which play a key role in the biological activities of Green Grass Jelly leaves.

The TLC profile of the ethanolic extract of Green Grass Jelly leaves (*C. barbata* Miers) is presented in **Figure 1**. Separation on silica gel F254 using n-hexane–ethyl acetate (5.5:4.5, v/v) produced several spots that showed different responses under visible light, UV light at 254 and 366 nm, and after derivatization. The appearance of spots following treatment with 10% H_2SO_4, Liebermann–Burchard reagent, and 5% $AlCl_3$ provided a preliminary indication of chemically diverse constituents, including steroid/triterpenoid- and flavonoid-like compounds. These TLC observations were consistent with the phytochemical screening results in **Table 2** and supported subsequent characterization by LC–HRMS.

In the third stage, the ethanolic extract of Green Grass Jelly leaves (*C. barbata* Miers) was monitored using Thin Layer Chromatography (TLC) on silica gel F254 plates, with the mobile phase optimized for optimal elution. The selected solvent system was chloroform: methanol (9:1). For qualitative detection of active compounds, three reagents were employed: 10% H_2SO_4 in methanol as a universal reagent, Liebermann–Burchard reagent for triterpenoids, and 5% $AlCl_3$ in methanol for flavonoids. This approach enabled the visualization and preliminary profiling of the extract's bioactive constituents.

In the fourth stage, the ethanolic extract of Green Grass Jelly leaves (*C. barbata* Miers) was analyzed using LC–HRMS. The chromatogram initially revealed 84 detected peaks. To refine the analysis, blank methanol peaks from the mobile phase were excluded, and duplicate compounds were removed, resulting in 44 tentatively identified peaks (**Figure 2**). The compounds were tentatively annotated based on accurate mass information and the retention times of targeted reference standards. Structural characterization of the 44 peaks was performed using accurate mass measurements, literature data, mass spectra, molecular weight, chemical formula, and fragmentation patterns. These were cross-checked against external databases, including MassBank, PubChem, ChemSpider, and relevant scientific journals. Although 84

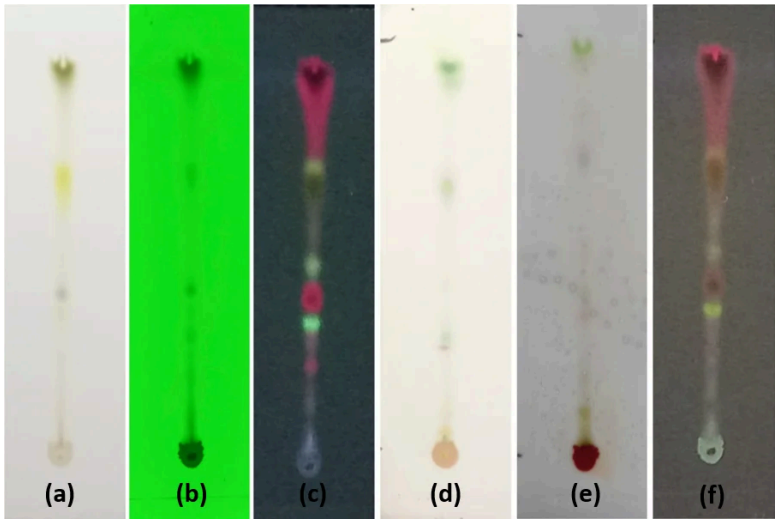

Figure 1. TLC profile of the ethanolic extract of Green Grass Jelly leaves, visualized under different conditions: (a) visual inspection, (b) UV light at 254 nm, (c) UV light at 366 nm, (d) 10% H_2SO_4 in methanol, (e) Liebermann–Burchard reagent, and (f) 5% $AlCl_3$ in methanol under UV 366 nm.

peaks appeared in the chromatogram, only those with identifiable literature-supported data were included in the final analysis. This approach ensures that the identified compounds are accurately characterized and relevant for further pharmacological evaluation.

Metabolites in the ethanolic extract of Green Grass Jelly leaves (*C. barbata* Miers) were successfully identified using LC–HRMS, as visualized in the Total Ion Chromatogram (TIC) in negative ion mode, with detailed compound data presented in **Supplemental Table 1**. Each peak in the chromatogram represents a compound eluted from the chromatography column at a specific retention time (RT). The varying peak intensities along the y-axis reflect the relative abundance of the detected ions. The highest peak was observed at RT 1.136 min, corresponding to 1, 3, 4, 5-Tetrahydroxycyclohexanecarboxylic acid, while other significant peaks appeared at RT 1.097 min and 26.664 min, identified as 2-C-methylerythritol 4-phosphate and Pheophorbide A, respectively. The diverse distribution of RTs and peak intensities highlights the complexity and richness of bioactive metabolites in the extract. The use of negative ion mode enhanced the sensitivity for detecting phenolic and flavonoid compounds. This TIC serves as a fundamental reference for compound annotation and supports qualitative metabolite analysis, providing a detailed chemical fingerprint crucial for phytopharmaceutical exploration.

LC–HRMS analysis resulted in the tentative annotation of 44 metabolites after data filtering and removal of duplicate features. Because compound assignment was based primarily on accurate mass measurements, isotopic patterns, database matching, and fragmentation similarity rather than authentic reference standards, the reported identities should be interpreted as putative rather than definitive identifications. Four major peaks were selected for further analysis based on their fragmentation profiles. This approach allows for interpretation of the fragment ions generated from each molecule, thereby strengthening the structural prediction of the compounds. For simplicity, the code "s" is used to represent each compound.

The first peak, with a retention time of 1.136 min and a mass of 192.063 ($C_7H_{12}O_6$), displayed a fragmentation pattern characterized by the loss of hydroxyl and carboxyl groups. This aligns with the predicted compound 1, 3, 4, 5-Tetrahydroxycyclohexanecarboxylic acid, which is rich in polar functional groups and prone to dehydration fragmentations. The s peak, at a retention time of 1.097 min and a mass of 216.039 ($C_5H_{13}O_7P$), exhibited characteristic phosphate-derived fragment ions in negative mode, supporting its identification as 2-C-methylerythritol 4-phosphate, a metabolite in the non-mevalonate pathway.

The third peak, with a retention time of 1.219 min and a mass of 210.073 ($C_7H_{14}O_7$), exhibited a fragmentation pattern characterized by successive losses of water molecules, a common behavior for sugars or carbonyl derivatives. This pattern supports the identification of Hept-2-ulose, a ketose compound with a strong tendency toward dehydration reactions.

Meanwhile, the fourth peak, observed at 26.66 min with a mass of 592.2666 ($C_{35}H_{36}N_4O_5$), displayed a fragmentation pattern typical of chlorophyll derivatives, including the loss of the phytol group or cleavage of the porphyrin ring. These fragments are consistent with the structure of Pheophorbide A, which contains a complex tetrapyrrole core. Collectively, the observed fragmentation patterns provide supporting evidence for the proposed annotations. However, because structural confirmation using authentic standards was not performed, the assignments remain tentative and should be interpreted with caution. Additional MS/MS comparison with reference compounds or NMR characterization would be required for definitive structural confirmation. In the fifth stage, molecular docking simulations of the test ligands against the target protein were performed using the PyRx application. The grid box was configured based on the size and active site of the protein as determined from prior validation. Adjustments were made to match the active site, setting the grid dimensions to 60 × 44 × 44 at the binding site coordinates.

In molecular docking, the grid box defines a 3D volume in which the docking algorithm searches for potential binding positions to optimize interactions between the ligand and the target. Its size and location are determined based on the dimensions of the target molecule and the ligand being tested. Proper adjustment ensures that the ligand can fully access the binding site, maintaining flexibility and allowing accurate prediction of ligand–protein interactions without spatial constraints.

Molecular docking simulations can analyze the position of a ligand relative to its target and the chemical bonds formed, allowing prediction of the ligand's affinity for the target. Docking of the test ligands was performed to determine their interactions and binding affinity with

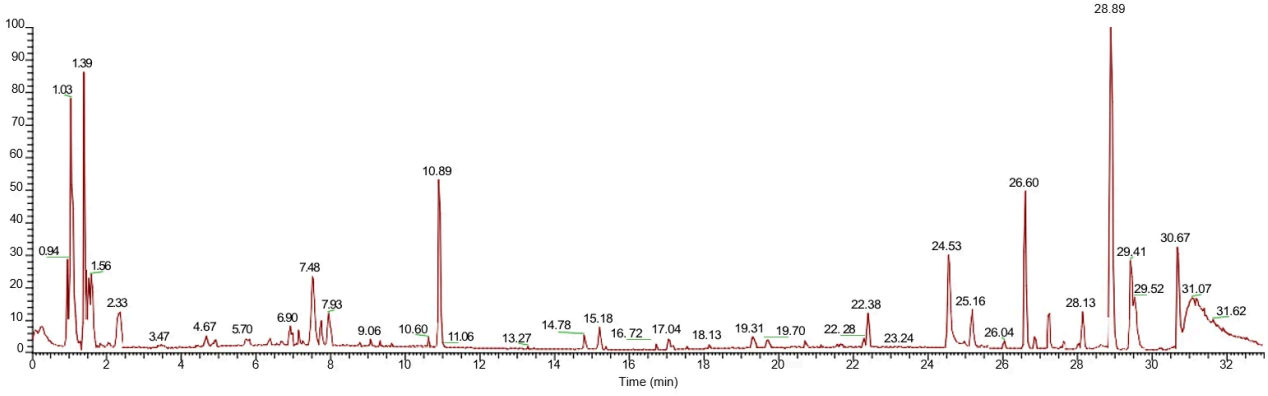

Figure 2. LC–HRMS chromatogram of the ethanolic extract of Green Grass Jelly leaves.

the active site of the target protein. The free binding energy (ΔG) is a measure of a ligand's ability to bind to a target: the lower (more negative) ΔG, the stronger the predicted binding affinity and conversely, higher ΔG values indicate weaker binding (16). ΔG values reflect the stability of the ligand–receptor complex; the more negative the ΔG, the more stable the interaction and the stronger the binding between the ligand and receptor (17, 18). Low free binding energy indicates a stable ligand–target complex (19). All the docking outputs can be seen in **Supplemental Table 2**.

Binding affinity values obtained from molecular docking provide an estimate of the thermodynamic favorability of protein–ligand interactions. However, docking scores should not be interpreted as direct measures of biological activity because cellular efficacy depends on multiple factors, including membrane permeability, metabolic stability, target selectivity, and downstream signaling responses. Therefore, the docking results presented here should be regarded as a preliminary screening tool for identifying compounds with potentially favorable interactions toward ERα. The corresponding

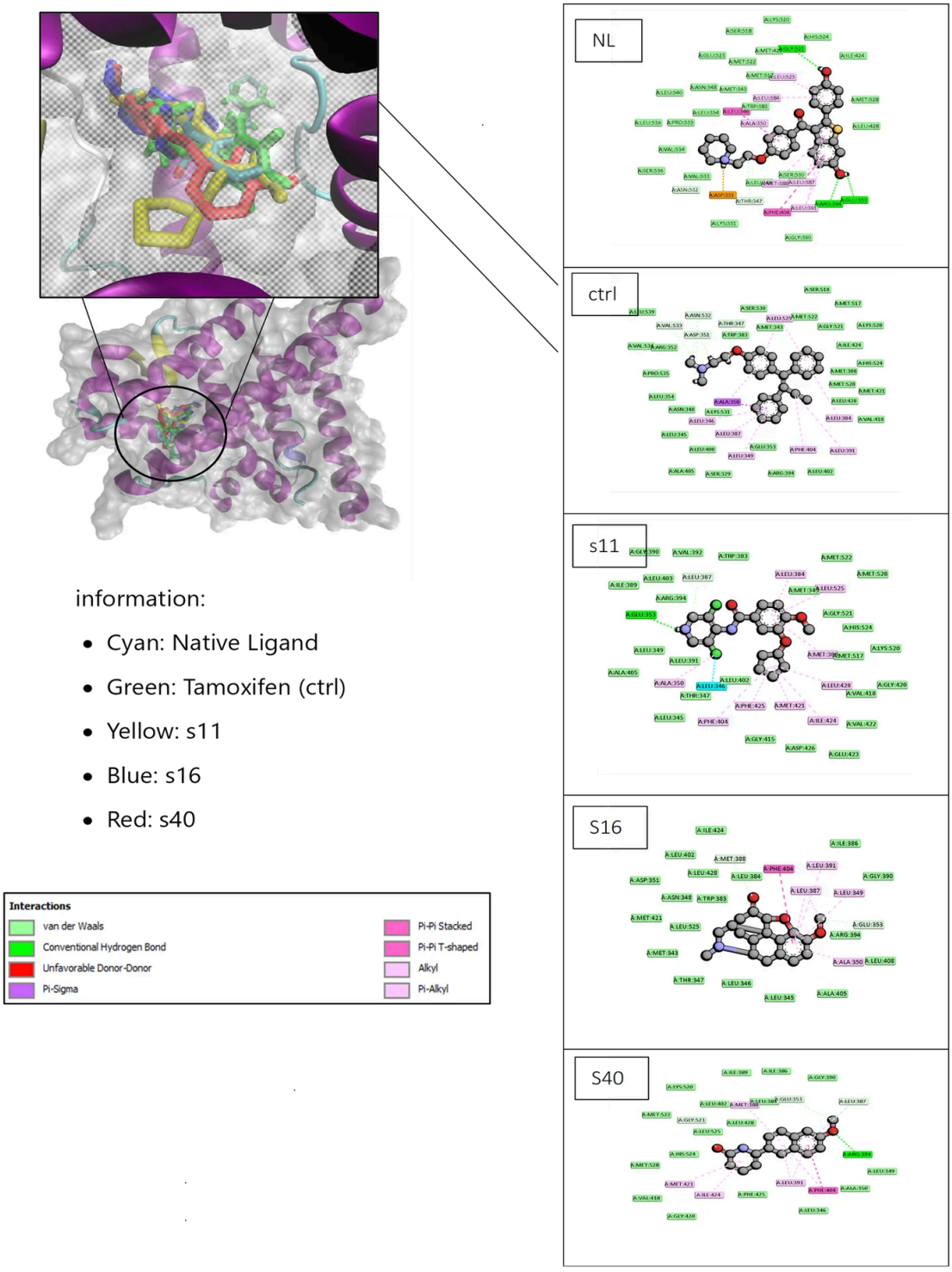

Figure 3. Ligand–protein docking visualization of Estrogen Receptor Alpha, showing the native ligand (NL), control (Tamoxifen; CTRL), and test compounds (s11, s16, and s40).

binding poses and residue-level interactions of the native ligand, tamoxifen, s11, s16, and s40 are presented in **Figure 3**.

Although compound s16 exhibited a more favorable docking score than tamoxifen, this result should be interpreted cautiously. Docking scores alone do not establish superior pharmacological activity. Tamoxifen is a clinically validated selective estrogen receptor modulator whose biological effects arise not only from receptor binding but also from specific conformational changes induced upon receptor interaction. Therefore, differences in docking scores do not necessarily translate into superior therapeutic efficacy. Nevertheless, the overlap of several binding-site residues suggests that s16 may interact within a similar region of the receptor and warrants further investigation.

The native ligand (NL) exhibited the highest binding affinity at –14.41 kcal/mol, forming five hydrogen bonds with key residues Arg394, Glu353, and Gly521, as well as eleven hydrophobic interactions involving Leu, Ala, and Phe residues. These results indicate that NL can stabilize the complex through a combination of polar and hydrophobic interactions, resembling or even surpassing the control ligand. Additionally, compounds s16 ((3β, 24R, 24′R)-fucosterol epoxide), s30 (3, 4a, 5-Trimethyl-6-{[(2E)-3-(methylsulfanyl)-2-propenoyl]oxy}-4,4a,5,6,7,8,8a,9-octahydronaphtho [2,3-b]furan-4-yl (2E)-2-methyl-2-butenoate), and s40 (6-(1,2,3,4-Tetrahydro-6-methoxy-2-naphthyl)-2 (1H)-pyridone) also demonstrated high binding affinities of –11.07, –9.46, and –8.09 kcal/mol, respectively, with varying residues involved within the active site pocket. These results suggest predicted favorable interactions of these compounds with Estrogen Receptor Alpha.

In the fifth stage, molecular dynamics (MD) simulations were conducted on the native ligand, Tamoxifen (CTRL), and the three top compounds: s11 (Piclamilast), s16 ((3β,24R,24′R)-fucosterol epoxide), and

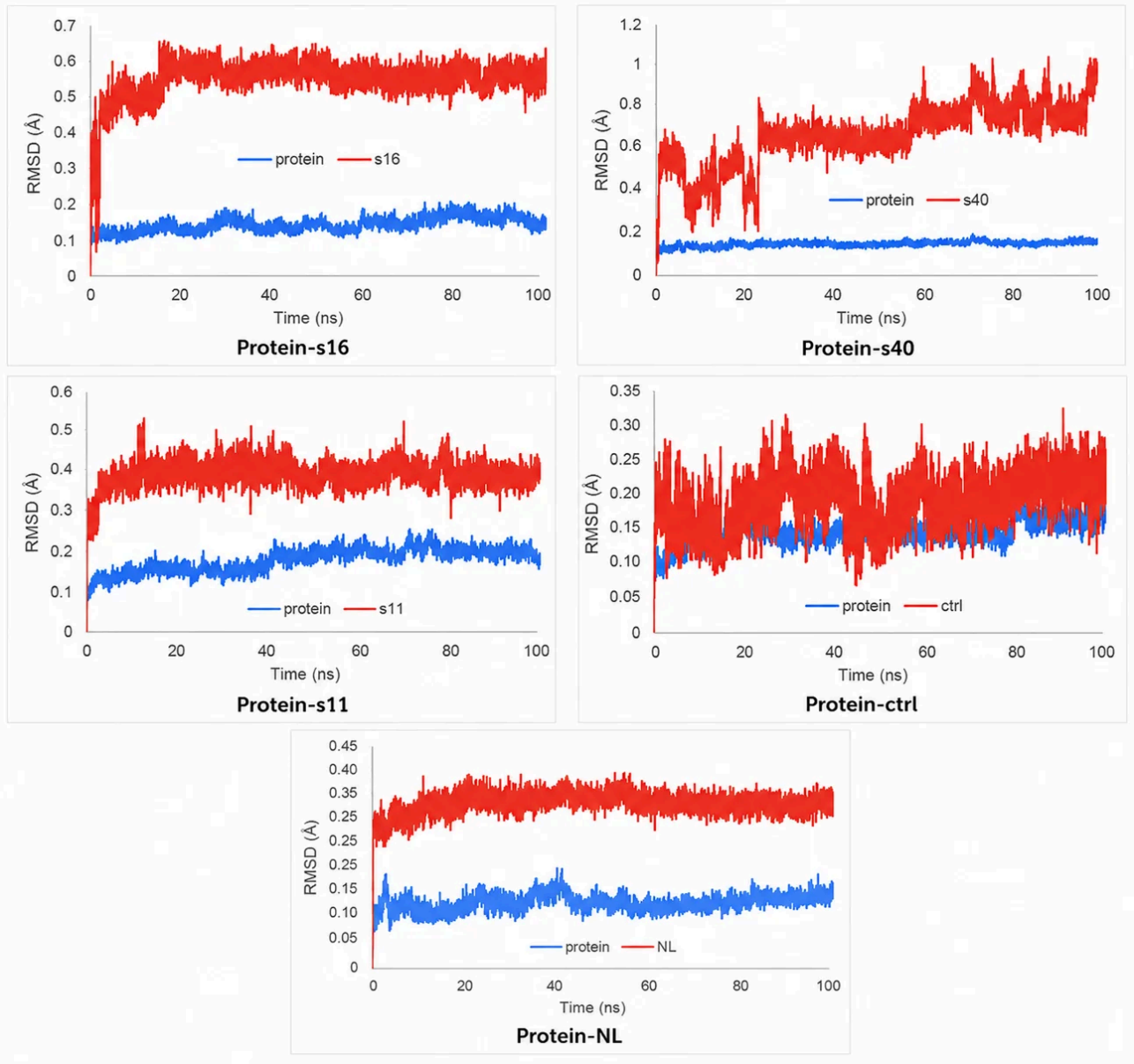

Figure 4. Root Mean Square Deviation (RMSD) of the protein–ligand complexes, comparing the native ligand (NL), control (tamoxifen; CTRL), and test compounds (s11, s16, and s40).

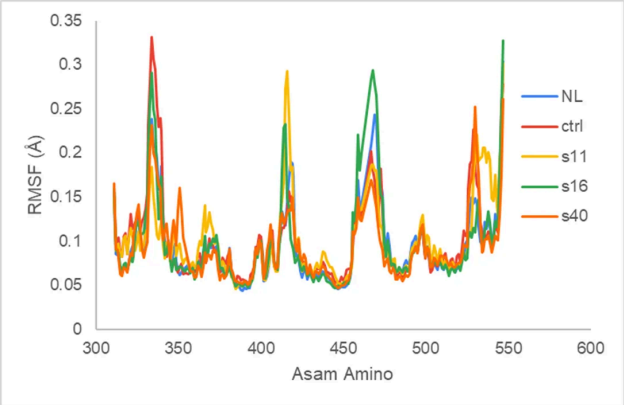

Figure 5. Residue fluctuations of Estrogen Receptor Alpha around the binding site atoms, comparing the native ligand (NL), control (tamoxifen; CTRL), and test compounds (s11, s16, and s40).

s40 (6-(1,2,3,4-Tetrahydro-6-methoxy-2-naphthyl)-2 (1H)-pyridone). These simulations were used to evaluate the stability of ligand interactions within the binding pocket of the target protein under conditions resembling physiological environments over a defined period. Topology and coordinate files for each ligand–protein complex were generated, and each system was solvated using the TIP3P water model with a 10 Å buffer around the protein. The complexes underwent energy minimization, followed by gradual heating to 310 K at 1 atm pressure, then equilibration and production phases running for 100 ns. After the simulations, analyses were performed on parameters including RMSD (Root Mean Square Deviation), RMSF (Root Mean Square Fluctuation), hydrogen bonds, SASA (Solvent Accessible Surface Area), radius of gyration (Rg), and MM-GBSA binding energy. These evaluations provided detailed insights into the stability, flexibility, and binding strength of the ligand–protein complexes over time.

RMSD (Root Mean Square Deviation) is a parameter used in molecular simulations to measure the degree of structural deviation of a molecule from its reference structure over the course of the simulation. RMSD is calculated as the average root mean square of the distances between corresponding atoms in two structures, typically comparing the initial structure to the structure at a given time point during the simulation. It reflects changes in atomic positions or fluctuations occurring at the active site of the target protein throughout the simulation. RMSD values below 2.0 Å to 5.0 Å indicate that the ligand remains stable within the binding pocket over the 100 ns simulation period (20). The RMSD profiles of the native ligand, tamoxifen, s11, s16, and s40 complexes are presented in **Figure 4**.

Molecular dynamics simulations were performed to evaluate the stability of the protein–ligand complexes based on Root Mean Square Deviation (RMSD) analysis. For the NL, CTRL, s11, s16, and s40 ligands, RMSD values of the protein 7NDO and the native ligand (NL) were monitored over 100 ns. The protein RMSD showed minor fluctuations, with an average value below 0.35 nm, indicating that the protein structure remained stable throughout the simulation. The NL, CTRL, and s11 (Piclamilast) ligands exhibited stable RMSD values between 0.2–0.5 Å over the 100 ns simulation period.

Ligand s16 ((3β, 24R, 24′R)-fucosterol epoxide) showed the highest fluctuation around 20 ns with an RMSD of 0.6 Å, which still indicates overall stability. In contrast, s40 (6-(1,2,3,4-Tetrahydro-6-methoxy-2-naphthyl)-2(1H)-pyridone) fluctuated more dynamically between 1–25 ns around 1 Å, then stabilized around 0.7 Å, but showed further fluctuations between 0.6–1.1 Å at 60 ns, suggesting some residual instability up to 100 ns. This indicates that although s40 experienced significant initial movement, its position eventually stabilized within the binding site. Overall, RMSD analysis provides critical insight into the structural stability of the complexes during simulation and serves to confirm that ligands can interact consistently with the protein over an extended period.

RMSF (Root Mean Square Fluctuation) is a metric that measures how much a specific particle, such as a protein residue, deviates from its reference position over a certain period, typically the average position of the particle over time (20). RMSF analysis identifies which structural components deviate the most or the least from their average structure. It evaluates the movements of individual atoms or amino acid residues that make up the receptor, reflecting the flexibility of the receptor. Overall, RMSF values indicate the displacement of each amino acid residue during the simulation, particularly at the active site, and provide insight into the flexibility and dynamic interactions of the protein–ligand complex. The residue-wise RMSF profiles of the simulated complexes are presented in **Figure 5**.

The Root Mean Square Fluctuation (RMSF) analysis of the Estrogen Receptor Alpha (ERα) complexes showed that the residues around the ligand binding site remained relatively stable, with RMSF values below 0.3 Å. The highest fluctuation was observed near residue Glu353, which plays a key role in hydrogen bonding with the native ligand. Low RMSF values at critical residues such as Arg394 and Gly521 indicate that the binding site remained stable throughout the simulation, demonstrating that the ligand–receptor complexes maintained good structural stability.

Furthermore, the similar fluctuation patterns observed between the control ligand (CTRL) and the test ligands (s11 (Piclamilast), s16 ((3β,24R,24′R)-fucosterol epoxide), s40 (6-(1,2,3,4-Tetrahydro-6-methoxy-2-naphthyl)-2(1H)-pyridone)) as well as the native ligand (NL) indicate that ligand binding did not induce major conformational changes in the receptor's active site. This suggests that interactions between the ligands and key residues in the binding pocket are strong enough to maintain the protein's configuration throughout the simulation. The low RMSF values observed for residues surrounding the binding pocket suggest limited local conformational changes during the simulation. However, because RMSF reflects residue flexibility rather than binding strength directly, these observations should be interpreted as supportive evidence of structural stability rather than definitive proof of ligand efficacy.

This analysis was performed to calculate the binding free energy between macromolecules and ligands using the MM-GBSA approach, which combines molecular mechanics calculations with a continuum solvation model. The gas-phase free energy (ΔG_gas) is calculated based

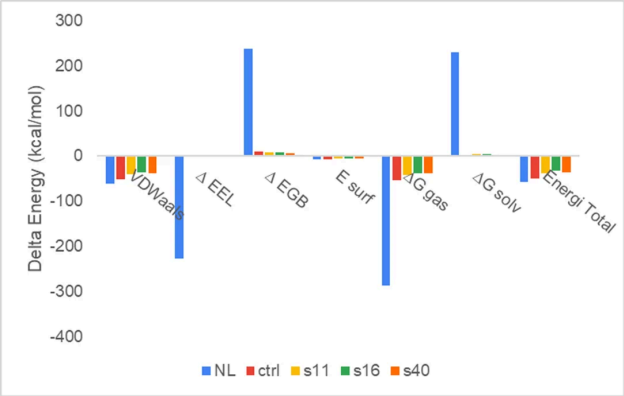

Figure 6. MM-GBSA binding energy calculations for the native ligand (NL), control (tamoxifen; CTRL), and test compounds (s11, s16, and s40).

primarily on van der Waals interactions (ΔE_VDW), which are typically more dominant than electrostatic energy contributions (ΔE_EL). Meanwhile, the solvation contributions are calculated using the Generalized Born model, where the polar solvation energy (ΔE_GB) and the non-polar surface energy (E_surf) contribute to the total solvation free energy (ΔG_solv). The final total binding free energy for each protein–ligand complex is obtained by summing ΔG_gas and ΔG_solv. The resulting energy components and total binding-energy estimates are presented in **Figure 6**.

In molecular dynamics simulations, MM-GBSA (Molecular Mechanics Generalized Born Surface Area) calculations are often used to estimate the binding strength between proteins and ligands. This method computes the total binding energy based on several components, including van der Waals energy (E_VDW), electrostatic energy (ΔE_EL), polar solvation energy (ΔE_GB), and non-polar solvation energy (E_surf). Using this approach, protein–ligand interactions can be analyzed more comprehensively and efficiently without the need to directly calculate free energy from long simulations.

The main purpose of MM-GBSA calculations is to determine the stability of the formed complex. The total binding energy is calculated as the sum of gas-phase energy (ΔG_gas = E_VDW + ΔE_EL) and solvation energy (ΔG_solv = ΔE_GB + E_surf). More negative total energy values indicate a more stable complex with stronger likely interactions. Based on MM-GBSA calculations, the complex between the native ligand (NL) and Estrogen Receptor Alpha exhibited the lowest total energy at –57.44 kcal/mol. This value indicates the most favorable estimated binding free energy among the simulated complexes. However, MM-GBSA calculations provide an approximation of relative binding energetics and should not be considered a direct predictor of biological potency. The primary contributors to complex stability were van der Waals interactions (–60.2 kcal/mol) and electrostatic energy (ΔE_EL = –227.44 kcal/mol), which play a major role in maintaining non-covalent interactions within the binding site. The negative ΔG_gas also indicates that the interatomic interactions within the complex occur spontaneously and are energetically favorable.

Meanwhile, the control ligand and test ligands (s11 (Piclamilast), s16 ((3β, 24R, 24'R)-fucosterol epoxide), and s40 (6-(1,2,3,4-Tetrahydro-6-methoxy-2-naphthyl)-2(1H)-pyridone)) showed higher total energy values compared to NL, at –49.00, –38.11, –31.96, and –36.77 kcal/mol, respectively. This indicates that the complex formed by the native ligand (NL) is more stable than those formed by the other ligands. The positive solvation energy contribution (ΔG_solv) in all complexes reflects energy compensation from the aqueous solvent environment, but it is not sufficient to offset the stabilizing effect of internal interactions within the complex. Therefore, it can be concluded that NL exhibits the strongest and most stable binding to Estrogen Receptor Alpha based on MM-GBSA energy calculations.

Conclusion

LC–HRMS analysis of the ethanolic extract of grass jelly leaves detected 84 chromatographic peaks. After blank subtraction and removal of duplicate features, 44 putatively identified compounds were retained for further analysis. Molecular docking against Estrogen Receptor Alpha (ERα) revealed that compounds s11 (Piclamilast), s16 ((3β, 24R, 24'R)-fucosterol epoxide), and s40 (6-(1,2,3,4-Tetrahydro-6-methoxy-2-naphthyl)-2(1H)-pyridone) exhibited favorable predicted binding affinities and interactions with several key residues involved in ligand recognition, including Arg394, Glu353, and Gly521. Subsequent molecular dynamics simulations suggested that the s11 and s16 complexes maintained relatively stable interactions within the receptor binding pocket throughout the simulation period.

However, these findings are based solely on computational analyses and putative metabolite identification, and therefore should be interpreted with caution. Binding affinity values, molecular dynamics parameters, and MM-GBSA energies provide only predictive information regarding protein–ligand interactions and do not constitute direct evidence of biological activity or therapeutic efficacy. Consequently, the present study identifies s16 as a compound of interest for further investigation rather than as a validated lead compound.

Declaration

Author Information

Abdul Mulki Irpani
*Corresponding author
Universitas Bhakti Kencana.
Contribution: Conceptualization, Methodology, Project administration, Validation, Writing - Original Draft.

Anne Yuliantini
Universitas Bhakti Kencana.
Contribution: Project administration.

Muhammad Ilham Bintang
Universitas Bhakti Kencana.
Contribution: Methodology, Software, Visualization.

Arinda Tri Pramay Sella
Universitas Bhakti Kencana.
Contribution: Methodology, Resources, Visualization.

Jajang Japar Sodik

Universitas Bhakti Kencana.
Contribution: Writing - Review & Editing.

Conflict of Interest
The authors declare no conflicting interest.

Data Availability
Data supporting the findings of this study are available from the corresponding author upon reasonable request.

Ethics Statement
Ethical approval was not required for this study.

Funding Information
This work was supported by the Direktorat Riset dan Pengabdian Masyarakat, Universitas Bhakti Kencana under Grant Number [054/02.PPM/UBK/VI/2025].

Supplementary Material
Supplementary Table 1 and **Supplementary Table 2** are provided in a single Microsoft Word document. The file can be downloaded from the journal's website via the following link.

References
1. Almalki SG. The pathophysiology of the cell cycle in cancer and treatment strategies using various cell cycle checkpoint inhibitors. Pathology - Research and Practice. 2023;251:154854. doi: https://doi.org/10.1016/j.prp.2023.154854

2. Mathur G, Nain S, Sharma P. Cancer: an overview Cancer: An Overview. Acad J Cancer Res [Internet]. 2015; 8 (1): 1–9. Available from: https://www.researchgate.net/publication/298789454_cancer_an_overview

3. Rezi E. Hubungan tingkat pengetahuan remaja putri tentang kanker payudara dengan pemeriksaan payudara sendiri (sadari) di sma negeri 12 padang. kebidanan. 2021;10(1):1-7. doi: https://doi.org/10.35328/kebidanan.v10i1.1064

4. Rahma RR. Evaluasi penggunaan obat tradisional berdasarkan dimensi ketepatan pemilihan obat. jkm. 2023;7(1):28-40. doi: https://doi.org/10.58554/jkm. v7i1.35

5. Shrihastini V, Muthuramalingam P, Adarshan S, Sujitha M, Chen JT, Shin H, *et al.* Plant Derived Bioactive Compounds, Their Anti-Cancer Effects and *In Silico* Approaches as an Alternative Target Treatment Strategy for Breast Cancer: An Updated Overview. Cancers. 2021;13(24):6222. doi: https://doi.org/10.3390/cancers13246222

6. Puspita Sari DRA. Uji toksisitas ekstrak etanol 96 % daun cincau hijau (Cyclea barbata Miers) terhadap Artemia salina Leach. dengan metode Brine Shrimp Lethality Test (BSLT). Journal Pharmactive. 2024;3(1):8-15. doi: https://doi.org/10.64036/pharmactive.v3i1.47

7. Santoso SS. Peran flavonoid cincau hijau (Premna oblongifolia) terhadap tumor otak. Pros Pertan dan Tanam Herb berkelanjutan di Indones [Internet]. 2017;53–61. Available from: https://jurnal.umj.ac.id/index.php/semnastan/article/view/2258

8. Millan-Casarrubias EJ, García-Tejeda YV, González-De la Rosa CH, Ruiz-Mazón L, Hernández-Rodríguez YM, Cigarroa-Mayorga OE. Molecular Docking and Pharmacological *In Silico* Evaluation of Camptothecin and Related Ligands as Promising HER2-Targeted Therapies for Breast Cancer. Cimb. 2025;47(3):193. doi: https://doi.org/10.3390/cimb47030193

9. Agu PC, Afiukwa CA, Orji OU, Ezeh EM, Ofoke IH, Ogbu CO, *et al.* Molecular docking as a tool for the discovery of molecular targets of nutraceuticals in diseases management. Sci Rep. 2023;13(1):1-18. doi: https://doi.org/10.1038/s41598-023-40160-2

10. Pharmawati M, Wirasiti NN, Wrasiati LP. Genotoxic and antigenotoxic potential of encapsulated Enhalus acoroides (L. f.) Royle leaves extract against nickel nitrate. Caryologia. 2022;75(2):89-99. doi: https://doi.org/10.36253/caryologia-1571

11. Julaiha, Widodo GP, Herowati R. Predicting ADME and Molecular Docking Analysis of Andrographis paniculata and Strobilanthes crispus Chemical Constituents Againts Antidiabetic Molecular Targets. J. Idn. Chem. Soc. 2019;2(2):106.doi: https://doi.org/10.34311/jics.2019.02.2.106

12. Kusriani H, Purwaniati P, Bintang MI. *In silico* study of Sambiloto (Andrographis paniculata) compounds from GC-MS and LC-MS/MS as alpha-glucosidase and DPP-4 enzyme inhibitor. Pharmaciana. 2024;14(3):443-456. doi: https://doi.org/10.12928/pharmaciana.v14i3.26643

13. Lestari SM, Camelia L, Rizki WT, Pratama S, Khutami C, Amelia A, *et al.* hytochemical Analysis and Determination of MIC and MFC of Cacao Leaves Extract (Theobroma cacao L.) against Malassezia furfur. J Jamu Indo. 2024;9(2):53-66. doi: https://doi. org/10.29244/jji.v9i2.316

14. Darusman F, Fakih TM. Studi Interaksi Senyawa Turunan Saponin dari Daun Bidara Arab (Ziziphus spina-christi L.) sebagai Antiseptik Alami secara *In Silico*. J Sains Farm Klin. 2020;7(3):233. doi: https://doi.org/10.25077/jsfk.7.3.233-239.2020

15. Rifai G, Rai Widarta IW, Ayu Nocianitri K. Pengaruh jenis pelarut dan rasio bahan dengan pelarut terhadap kandungan senyawa fenolik dan aktivitas antioksidan ekstrak biji alpukat (persea americana mill.). itepa. 2018;7(2):22. doi: https://doi.org/10.24843/itepa.2018.v07.i02.p03

16. Rasyid H, Mardiyanti R, Arief I, Saputri WD. An Insight of Cryptocarya Secondary Metabolites as Anticancer P388: Study of Molecular Docking and ADMET Properties. molekul. 2023;18(1):89. doi: https://doi.org/10.20884/1.jm.2023.18.1.6364

17. Syarafina ZYI, Safithri M, Bintang M, Kurniasih R. *In Silico* Screening of Cinnamon (Cinnamomum burmannii)

Bioactive Compounds as Acetylcholinesterase Inhibitors. J. Kim. Sains Apl. 2022;25(3):97-107. doi: https://doi.org/10.14710/jksa.25.3.97-107

18. Zheng X, Polli J. Identification of inhibitor concentrations to efficiently screen and measure inhibition Ki values against solute carrier transporters. European Journal of Pharmaceutical Sciences. 2010;41(1):43-52. doi: https://doi.org/10.1016/j.ejps.2010.05.013

19. Hairulazam A, Malaysia U, Sultan J, Shah A, Samian IA, Azzar A, *et al*. *In Silico* Docking of Epicatechin, Corilagin and Quercetin as Potential Pancreatic Lipase Inhibitor for Obesity Treatment. Int J Allied Heal Sci. 2021;5(2):2194–200.

20. Asnawi A, Febrina E, Aligita W, Yuliantini A, Arfan A. Penambatan Molekul dan Dinamika Molekul beberapa Fitokimia dari Acalypha Indica L. sebagai Inhibitor Matriks Metalloproteinase9. J Sains Farm Klin. 2023;10(1):62. doi: https://doi.org/10.25077/jsfk.10.1.62-70.2023

Additional Information

How to Cite

APA 7th Edition: Irpani, A. M., Yuliantini, A., Bintang, M. I., Pramay Sella, A. T. & Sodik, J. J. (2026). Ethanol Extract of Grass Jelly Leaves: Bioactive Analysis and In silico Study on Estrogen Receptor Alpha Related to MCF-7 Breast Cancer. Sciences of Pharmacy, 5(3), 312-322. https://doi.org/10.58920/sciphar0502619

Vancouver: Irpani AM, Yuliantini A, Bintang MI, Pramay Sella AT, Sodik JJ. Ethanol Extract of Grass Jelly Leaves: Bioactive Analysis and In silico Study on Estrogen Receptor Alpha Related to MCF-7 Breast Cancer. Sciences of Pharmacy. 2026;5(3):312-322. https://doi.org/10.58920/sciphar0502619

Harvard: Irpani, A. M., Yuliantini, A., Bintang, M. I., Pramay Sella, A. T. & Sodik, J. J. (2026) 'Ethanol Extract of Grass Jelly Leaves: Bioactive Analysis and In silico Study on Estrogen Receptor Alpha Related to MCF-7 Breast Cancer', Sciences of Pharmacy, 5(3), pp. 312-322. doi: 10.58920/sciphar0502619

Publisher Note

Open Access